IR spectral and structural changes caused by the conversion of salophen into oxyanion and dianion

S. Stoyanov, E. Velcheva, B. Stamboliyska*

Institute of Organic Chemistry, Centre of Phytochemistry, Bulgarian Academy of Sciences, Acad. G. Bonchev Str. Bl. 9, Sofia, 1113, Bulgaria

The structures of salophen molecule its oxyanion and dianion have been studied by means of both IR spectra and DFT calculation, employing the B3LYP functional and 6-311++G** basis set. The solvent effect was simulated by using self-consistent the integral equation formalism variant (IEFPCM) model. A good agreement has been found between the theoretical and experimental vibrational characteristic of the particles studied. The theoretical method used gives a good description on the strong spectral changes caused by the conversion of the salophen into anion and dianion. The structural changes which accompany these conversions are also essential. Analysis of the atomic charge changes shows that the first (oxyanionic) charge remains localized mainly within the oxyphenylene fragment while the second (nitranionic) charge spreads mainly over the acetanilide fragment.

Keywords: IR; DFT; Acetaminosalol; Oxyanion; Dianion.

INTRODUCTION

Organic anions are key to many chemical and biological processes and their important role in the synthesis, design of functional materials and drugs induce numerous studies within the field of organic chemistry and all interfacing disciplines [*e.g.* 1–5]. A better knowledge of the structure of organic anions is an essential point in understanding the mechanism of their actions. However, the highly reactive nature of anionic species has limited their structural characterization. The conversions of neutral molecule into anions (oxyanions, carbanions, azanion, dianions, radical-anions, *etc.*) are accompanied by essential changes in the vibration spectra. So, these changes are very informative for the structural variations caused by the same conversions [6]. The structure of large series of organic molecules and their anions have been successfully studied recently on the basis of experimental IR spectra combined with DFT/ computations [7–13]. The title compound is an interesting and convenient object of the molecule → anion→ dianion conversion investigations, as it contains (–OH) and (-CO-NH-) acidic functional groups and can be converted successively into oxyanion and dianion.

Salophen (Phenetsal, Acetaminosalol, (4-acetamidophenyl) 2-hydroxybenzoate) is an ester of salicylic acid and acetaminophenol, used as an antirheumatic, antipyretic, analgesic and intestinal antiseptic [14]. Due to its antimicrobial function, salophen is used as an ingredient in cosmetic products, pharmaceutical compositions, surgical materials, *etc.* [15]. Crystal structure of salophen was recently determined experimentally [16]. Its IR spectra in KBr are included in many databases [14]. Infrared linear dichroic and Raman spectroscopic approach for determination of salophen in binary solid mixtures with caffeine was reported [17]. Neither the detailed IR spectra nor structure of oxyanion and dianion of salophen have been studied theoretically or experimentally. The purpose of the present investigation is to follow the spectral and structural changes, caused by the conversion of salophen molecule into the corresponding anions on the basis of both DFT computations and spectroscopic experiments. Its relative predictive capabilities are evaluated by comparing the theoretically predicted and experimentally frequencies measured in DMSO

EXPERIMENTAL AND COMPUTATION

Salophen (Sigma–Aldrich) was used without additional purification. The salophen anion was prepared by adding solutions of the parent compound in

* To whom all correspondence should be sent:
E-mail: bs@orgchm.bas.bg

dimethyl sulfoxide (DMSO) and DMSO-d_6 (Fluka) to equimolar quality of dry alkali-metal methoxides and methoxides-d_3. The suspensions obtained were stirred for 1 min and then filtered through a siringe-filter. The conversion was practically complete (Fig. 1(A) and Fig. 1(B)). The dianion salophen was prepared by reacting DMSO and DMSO-d_6 solutions of the parent compound with an excess of dry alkali-metal methoxides and methoxides-d_3. The conversion was also practically complete: in the spectra we found neither the bands of salophen nor those of its anion (cf. Fig. 1(A-C)). The IR spectra were recorded at a resolution of 1 cm^{-1}, by 64 scans on a Tensor 27 FTIR spectrophotometer in a CaF$_2$ cell of 0.13 mm path length for solutions, spectra of the solid state sample were obtained by ATR technique and in KBr pellet.
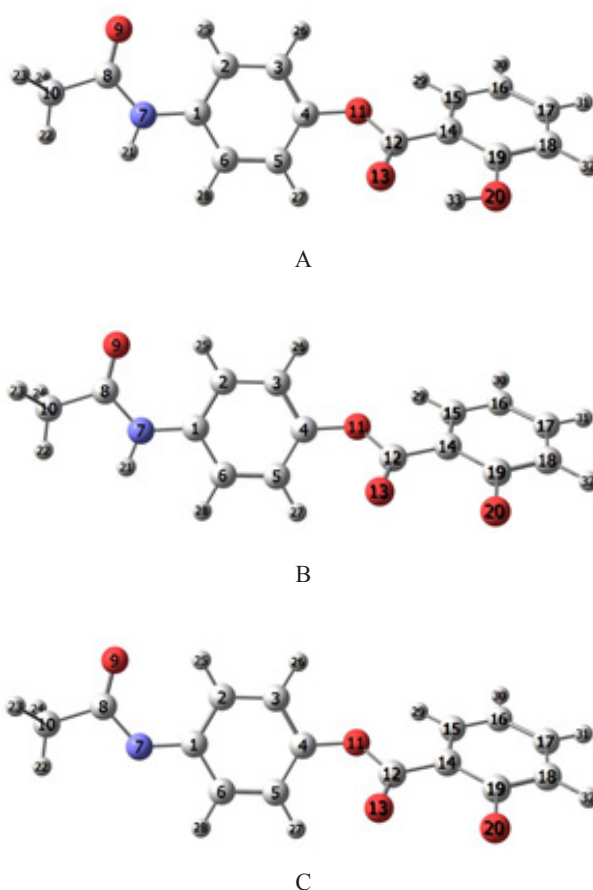
The quantum chemical calculations the Natural bond orbital (NBO) population analysis [18] were performed using the Gaussian 09 package [19]. The geometry optimizations of the structures investigated were done without symmetry restrictions, using density functional theory (DFT). We employed B3LYP hybrid functional, which combines Becke's three-parameter nonlocal exchange with the correlation functional of Lee et al. [20, 21], adopting 6-311++G** basis sets. To estimate the effect of the solvent (DMSO) on the infrared spectra of studied species, we applied the integral equation formalism of polarizable continuum model (IEFPCM), proposed by Tomasi and coworkers [22, 23]. The stationary points found on the molecular potential energy hypersurfaces were characterized using standard harmonic vibrational analysis. For a better correspondence between experimental and calculated values, we modified the results using the empirical scaling factors. The relative predictive capability of theoretical method used is evaluated by comparing the theoretically predicted and experimentally frequencies measured in DMSO.

RESULTS AND DISCUSSION

Energy analysis

All conformers of salophen and its deprotonated forms were determined from rotation about Ph-N, and N-C, C-O, C-CO bonds. The structures of the most stable conformers are shown in Scheme 1.

Both structures of molecule and anion correspond to *trans*-type conformers with respect to the NH and amide carbonyl groups and *cis*-type conformers with respect to hydroxyl and the ester carbonyl group. The presence of the same conformer for the molecule was also established by crystallographic analysis [16].

A

B

C

Scheme 1. B3LYP/6311++G** optimized structures of the most stable conformers of molecule A and its oxyanion B and dianion C.

The calculated total energies of the studied species are as follow:

E_{tot} = –935.3485099 H for the salophen molecule A
E_{tot} = –934.8173745 H for the salophen oxyanion B
E_{tot} = –934.1777714 H for the salophen dianion C.

The following deprotonation energies correspond to the above values (see also Scheme 1):

$E^d = E_{tot}(B) - E_{tot}(A) = 1394.230239$ kJ mol^{-1};
$E^d = E_{tot}(C) - E_{tot}(B) = 1668.595$ kJ mol^{-1}.

The energy difference E^d is related to the gas-phase Broensted acidities, and can be used as an approximate measure of these acidities in polar aprotic solvents [24]: low $E^d \rightarrow$ high acidities $\rightarrow$ low pKa values. For comparison, the first deprotonation energy is lower than E^d of acedoben (1448.1 kJ mol^{-1}), acetanilide (1489.06 kJ mol^{-1} [12]) and higher than E^d of the stronger acid acesulfame (1324.31 kJ mol^{-1}

[8], in agreement with the experimentally estimated pKa value of 7.87. The second deprotonation energy is essentially higher, and can be compared with the second deprotonation energy of acedoben (1734.1 kJ mol^{-1} [13]). This result is not surprising, having in mind that the products of the second deprotonation are in fact dianions.

Infrared analysis

Let us consider consecutively the IR data of the species studied, which will make it possible to specify the spectral changes, caused by the conversion of the salophen molecule into corresponding anions.

The experimental IR spectra of salophen, measured in DMSO-d$_6$ solution and in solid state (ATR) are shown in Fig. 1.

Based on the differences in the DMSO and solid state spectra in the carbonyl region, it could be assumed that two different forms are present – with and without intramolecular hydrogen bond. The strong intramolecular OH...O=C hydrogen bond existing in solid state produces a C=O ester stretching band with maximum at 1680 cm^{-1}. The DMSO as polar aprotic solvent usually decreases the frequencies of polar groups. But in IR spectra of salophen in solvent this ν(CO) band occurs at a higher frequency (1740 cm^{-1}, Fig. 1), because DMSO breaks the intramolecular hydrogen bond. For this reason

we compared the experimental vibrational characteristics with the calculated ones of conformer, in which the carbonyl group is not intramolecularly hydrogen bonded. It can be seen in Figure 1 that the amide band ν(C=O) is shifted in the solution with 26 cm^{-1}. The numerical values of experimental vibrational characteristics are listed together with the theoretical ones in Table 1. The agreement between the experimental and calculated values is very good – the mean absolute deviation between observed and calculated frequencies is 8.3 cm^{-1}, which value is not away from the lower border of the 8–16 cm^{-1} interval of deviations, typical for the DFT calculations for molecules containing carbonyl groups [8–13].

No experimental data for the ν(OH) and ν(NH) bands were given in the Table 1, as they form a multiplet because of the formation of hydrogen bonds mainly with the solvent. The assignment of the experimental bands to the calculated normal modes in the C–H stretching region (3100–2800 cm^{-1}) is not obvious because there are fewer bands in the experimental spectrum than predicted by the calculations. The highest frequency experimental bands observed in the IR spectrum (3200–3000 cm^{-1}) are assigned to the aromatic C–H stretches, while the lower frequency bands are attributed to the methyl group motions. The calculations resolved and located well the two carbonyl stretching vibrations, those
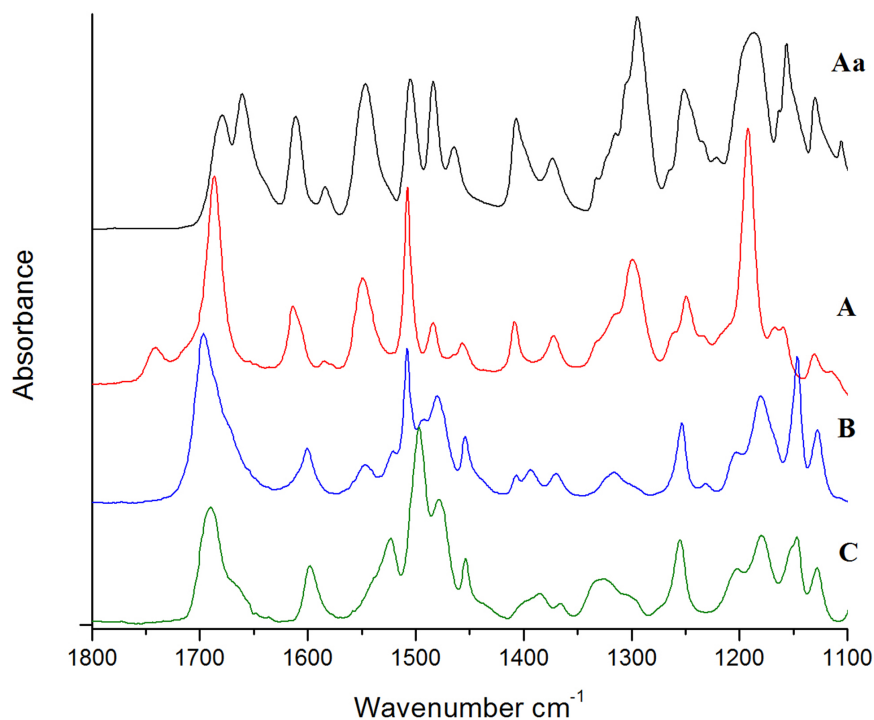

Fig. 1. ATR-FTIR spectrum of salophen (Aa); Infrared spectra of salophen (A), its oxyanion (B) and its dianion (C) in DMSO-d$_6$.

Table 1. Theoretical (B3LYP/6-311++G**) and experimental (solvent DMSO-d_6) vibrational frequencies (in cm^{-1}) and IR integrated intensities (A in km.mol^{-1}) of salophen

No.	$\nu_{calc.}$ [a]	A	Assignments	$\nu_{exp.}$
1.	1739	716.4	ν(C=O) (ester group)	1741
2.	1688	452.8	ν(C=O) (amide group)	1686
3.	1633	32.6	ν^{Ph}(CC), δ^{Ph}(CCH)	
4.	1629	147.3	ν^{Ph}(CC), δ^{Ph}(CCH)	1606
5.	1626	65.7	ν^{Ph}(CC), δ^{Ph}(CCH)	
6.	1609	62.2	ν^{Ph}(CC), δ^{Ph}(CCH)	1584
7.	1543	516.8	δ(HNC), ν(N-C)	1549
8.	1523	322.6	δ^{Ph}(CCH), ν^{Ph}(CC)	
9.	1515	106.5	δ^{Ph}(CCH), δ(HOC)	1507
10.	1473	26.7	δ(CH$_3$)	1483
11.	1466	89.4	δ^{Ph}(CCH), ν^{Ph}(CC)	1467
12.	1455	13.5	δ(CH$_3$)	1456
13.	1419	103.8	δ^{Ph}(CCH), δ(HNC)	1408
14.	1390	58.0	δ(CH$_3$)	
15.	1358	60.7	δ(HOC)	1372
16.	1331	155.7	ν(CN), ν^{Ph}(Ph-N)	1332
17.	1328	133.1	ν(Ph-OC), ν(C-OH)	1319
18.	1316	12.4	δ^{Ph}(CCH), δ(HNC)	
19.	1287	111.4	ν(C-OH)	1299
20.	1263	101.3	ν(C-CH$_3$), ν(Ph-N), ν(CN)	1263
21.	1236	250.7	δ^{Ph}(CCH), ν(Ph-CO)	1249
22.	1230	35.0	ν(Ph-N), δ(CH$_3$)	1233
23.	1194	753.0	ν(Ph-OC)	1192
24.	1192	68.1	δ^{Ph}(CCH), δ(HOC)	
25.	1177	21.0	δ^{Ph}(CCH), ν^{Ph}(CC)	1167
26.	1175	260.1	δ^{Ph}(CCH), ν^{Ph}(CC)	1159
27.	1133	228.4	δ^{Ph}(CCC), ν^{Ph}(CC)	1130
28.	1123	20.9	δ^{Ph}(CCC), ν^{Ph}(CC)	1116
29.	1061	29.9	δ^{Ph}(CCH), ν^{Ph}(CC)	

[a] Scaled by 0.993. [b] Vibrational modes: ν, stretching; δ, bendings. The numbers before the mode symbols indicate % contribution (10 or more) of a given mode to the corresponding normal vibration, according to the potential energy distribution.

of the ester and the amide groups, at 1739 cm^{-1} and 1688 cm^{-1}, respectively. The theory does not reproduce qualitatively well the high integral intensities for the carbonyl bands in the experimental spectrum. DFT calculations predicted well also the IR frequencies of the amide-II and amide-III vibrations measured in DMSO. The amide-II mode δ(HNC) is predicted to appear at 1544 cm^{-1} as a very intense band. Experimentally, a very strong band was detected at 1549 cm^{-1} in DMSO. The stretching ν(N-C) coupled with ν(Ph-N), denoted as amide-III was predicted and measured as an intensive band at 1332 cm^{-1}. The highest intensity band in the theoretical and experimental spectrum at 1192 cm^{-1} is assigned to ν(Ph-CO).

The experimental spectrum of salophen anion in DMSO solvent is shown in Fig. 1(B). It is known that in this solvent the ions exist as free species and there are no anion/counter ion interactions [25]. The

influence of the counterions on the frequencies is neglectful. This makes it possible to compare, in this work, the experimental infrared data for the anions with the theoretical ones. The numerical values of the experimental vibrational data in DMSO-d_6 are listed with the theoretical ones in Table 2.

As above we can find there a good agreement between experimental and scaled theoretical frequencies. The mean deviation between them is 5.6 cm^{-1}. In full agreement between theory and experiment, the conversion of the salophen molecule into the oxyanion is accompanied by an essential decrease in frequency of ester ν(CO) band: predicted 39 cm^{-1}, measured 45 cm^{-1} and has only a weak effect on the amide ν(CO) frequency: predicted decrease 4 cm^{-1}, measured 2 cm^{-1} (Tables 1 and 2; Fig. 1). The shifting between the two carbonyl frequencies expected in this case should amount to a 16 cm^{-1} and it is in agreement with the experimental measured after

Table 2. Theoretical (B3LYP/6-311++G** and experimental (solvent DMSO-d_6) vibrational frequencies (ν in cm^{-1}) and IR integrated intensities (A in km mol^{-1}) of salophen anion

No.	$\nu_{calc.}$ [a]	A	Assignments	$\nu_{exp.}$
1.	1700	1224.8	ν(C=O) (ester group)	1696
2.	1684	469.3	ν(C=O) (amide group)	1684
3.	1633	18.8	ν^{Ph}(CC), δ^{Ph}(CCH)	
4.	1622	83.8	ν^{Ph}(CC), δ^{Ph}(CCH)	
5.	1618	211.4	ν^{Ph}(CC), δ^{Ph}(CCH)	1601
6.	1540	535.9	δ(HNC), ν(N-C)	1546
7.	1529	192.7	δ^{Ph}(CCH)	1521
8.	1522	426.7	δ^{Ph}(CCH), ν^{Ph}(CC)	1508
9.	1483	604.8	ν(C-O$^-$)	1492
10.	1473	194.5	δ(CH$_3$)	1481
11.	1469	27.8	δ^{Ph}(CCH)	1470
12.	1455	13.4	δ(CH$_3$)	1454
13.	1418	91.9	δ^{Ph}(CCH), δ(HNC)	1406
14.	1389	57.8	δ(CH$_3$)	1393
15.	1389	48.3	δ^{Ph}(CCH)	1369
16.	1329	174.4	ν(CN), ν^{Ph}(CC)	1325
17.	1316	14.9	ν(Ph-OC)	1316
18.	1313	6.2	δ^{Ph}(CCH), δ(HNC)	
19.	1270	94.0	δ(HNC), δ(CH$_3$)	
20.	1258	147.0	δ^{Ph}(CCH)	1253
21.	1229	42.1	ν(Ph-N), δ(CH$_3$)	1231
22.	1215	218.7	ν(Ph-OC)	1202
23.	1179	56.3	δ^{Ph}(CCH), ν^{Ph}(CC)	1180
24.	1173	273.6	δ^{Ph}(CCH), ν^{Ph}(CC)	
25.	1153	508.7	δ^{Ph}(CCH), ν^{Ph}(CC)	1146
26.	1121	416.4	δ^{Ph}(CCH), ν^{Ph}(CC)	1127
27.	1120	197.8	δ^{Ph}(CCC), ν^{Ph}(CC)	
28.	1046	12.4	ν(C-CH3), δ(CH$_3$)	

[a] Scaled by 0.993. [b] Vibrational modes: ν, stretching; δ, bendings. The numbers before the mode symbols indicate % contribution (10 or more) of a given mode to the corresponding normal vibration, according to the potential energy distribution.

having decomposed the complex band into components (1696 cm^{-1}, 1684 cm^{-1}, Table 2). The conversion causes also an essential intensity increase of the ester carbonyl ν(CO) bands. In the spectrum of the anion the aromatic skeletal bands of the phenolate ring 8 and 19 (Wilson's notation) are more intense than these in the spectrum of neutral molecule. Conversion of the salophen molecule into the oxyanion virtually did not change the frequencies of δ(HNC) (amide-II) and ν(C-N) (amide-III) bands. Removing the proton from the hydroxyl group of the oxyanion leads to a shift of the ν (Ph–O) coordinate to higher frequency (1492 cm^{-1}), obviously due to the significant shortening of the Ph–O bond.

The experimental spectrum of the dianion studied is shown in Fig. 1(C). Theoretical and experimental IR data for the salophen dianion are compared in Table 3. Again, there is good agreement between experimental and scaled theoretical frequencies. The mean deviation between them is 9.1 cm^{-1}.

Comparison with the other spectra of Fig. 1(B) shows that fundamental spectral changes accompany the second deprotonation of salophen. There is no longer amide band ν(C=O) at the usual place. The theory predicts two new bands characterizing the carboxamide group in the dianion: very strong bands at 1524 cm^{-1} (amide I) and 1393 cm^{-1} (amide III). These bands are actually present in the experimental spectrum (Fig. 1(C)): i.e., at 1522 cm^{-1} and 1386 cm^{-1}. The approximate description of the corresponding normal vibrations (Table 3, No. 6 and 14) are in agreement with the literature data. For the nitranions of acetanilide and of a series of ring-substituted acetanilides, Ognyanova et al. have assigned the strong bands in the 1518–1533 cm^{-1} spectral region as ν(C=O) (amide I) and the medium to strong bands at 1373–1382 cm^{-1} – as ν(C-N) (amide III). In agreement between theory and experiment, the second deprotonation of salophen causes a strong enhancement of the intensity of the aromatic skel-

Table 3. Theoretical (B3LYP/6-311++G**) and experimental (solvent DMSO-d_6) vibrational frequencies (ν in cm^{-1}) and IR integrated intensities (A in km.mol^{-1}) of salophen dianion

No.	$\nu_{calc.}$ [a]	A	Assignments	$\nu_{exp.}$
1.	1706	1150.0	ν(C=O) (ester group)	1689
2.	1629	57.0	ν^{Ph}(CC), δ^{Ph}(CCH)	
3.	1625	182.8	ν^{Ph}(CC), δ^{Ph}(CCH)	
4.	1586	2.3	ν^{Ph}(CC), δ^{Ph}(CCH)	1599
5.	1539	216.3	ν^{Ph}(CC), δ^{Ph}(CCH)	
6.	1524	1018.9	ν(C=O), ν(N-C)	1522
7.	1506	808.6	δ^{Ph}(CCH), ν(Ph-N)	1496
8.	1487	641.7	ν(C-O$^-$)	1478
9.	1477	191.7	δ^{Ph}(CCH)	
10.	1471	10.2	δ(CH$_3$)	
11.	1456	198.5	δ(CH$_3$)	1454
12.	1425	40.7	δ^{Ph}(CCH)	
13.	1394	77.8	δ^{Ph}(CCH)	
14.	1393	643.1	ν(N-C), ν(C-CH3)	1386
15.	1363	88.1	δ(CH$_3$)	1366
16.	1321	29.0	ν(Ph-O-C)	1326
17.	1306	16.4	δ^{Ph}(CCH)	
18.	1292	12.2	δ^{Ph}(CCH)	1255
19.	1265	211.4	δ^{Ph}(CCH)	
20.	1225	6.2	ν(Ph-N), ν(C-CH$_3$)	
21.	1206	64.0	ν(Ph-OC)	1202
22.	1179	377.4	δ^{Ph}(CCH), ν^{Ph}(CC)	1179
23.	1163	10.5	δ^{Ph}(CCH), ν^{Ph}(CC)	
24.	1159	538.2	δ^{Ph}(CCH), ν^{Ph}(CC)	1464
25.	1128	612.9	δ^{Ph}(CCH), ν^{Ph}(CC)	1128
26.	1108	27.3	δ^{Ph}(CCH), ν^{Ph}(CC)	
27.	1046	4.4	δ(CH$_3$)	
28.	1041	51.0	δ^{Ph}(CCH)	
29.	1017	30.9	δ(CH$_3$)	
30.	1017	9.3	δ(CH$_3$)	

[a] Scaled by 0.993. [b] Vibrational modes: ν, stretching; δ, bendings. The numbers before the mode symbols indicate % contribution (10 or more) of a given mode to the corresponding normal vibration, according to the potential energy distribution.

etal bands of the phenylene ring 19 (Wilson's notation). This band is the strongest in the spectrum of the dianion.

Structural analysis of the species studied

According to both the X-ray diffraction experiment [16] and the DFT theory the salophen molecule is composed of atoms lying approximately in two planes: one of the phenylene ring and the carboxamide group, and the other of the salicylate fragment. The twisting angle has been experimentally found to be 93.5° [16]. The same angle for the isolated salophen molecule has been theoretically estimated at 95.5°. The corresponding values for the free salophen anion and dianion are 102.8° and 88.4°, respectively. The theoretical and experimental bond lengths and angles in the salophen and its oxyanion

and dianion are listed in Table 4. The conversion of salophen into the oxyanion leads to changes in all the bond lengths, but the strongest ones are the shortening of the C^{19}–O^{20} bond with ca. 0.089 Å and lengthening of the adjacent CC ones with ca. 0.048 Å. The C^{14}–C^{12} bond in the anion is with 0.024 Å shorter while the C^{12}–O^{11} bonds and the C=O^{13} bond are with 0.012 Å and 0.007 Å longer that the same bonds in the molecule. The bond length changes that accompany the conversion of the oxyanion into dianion take place both at the azanionic center and next to it – shortening of the C^1–N^7 and N^7–C^8 and bonds and lengthening of the C^8=O^9 and C^8–CH$_3$ bonds (Table 4).

The net electric charges of certain fragments of the species studied and the corresponding charge changes accompanying the conversion molecule → oxyanion → dianion are shown in Table 5.

Table 4. Theoretical (B3LYP/6-311++G**) and experimental bond lengths R (Å) and bond angles A (°) in the salophen, its oxyanion and dianion

	Molecule			Anion		Dianion	
	Experimental[a]	Theoretical	Δ^b	Theoretical	Δ^c	Theoretical	Δ^d
Bond lengths							
$R(C^1,C^2)$	1.397	1.403	−0.006	1.402	−0.001	1.419	−0.017
$R(C^2,C^3)$	1.389	1.388	0.001	1.395	0.007	1.396	−0.001
$R(C^3,C^4)$	1.384	1.390	−0.006	1.389	−0.001	1.389	0.000
$R(C^4,C^5)$	1.376	1.386	−0.010	1.395	0.009	1.393	0.002
$R(C^5,C^6)$	1.393	1.394	−0.001	1.389	−0.005	1.389	0.000
$R(C^6,C^1)$	1.395	1.403	−0.008	1.402	−0.001	1.418	−0.014
$R(C^1,N^7)$	1.414	1.411	0.003	1.413	0.002	1.394	0.019
$R(N^7,C^8)$	1.357	1.370	−0.013	1.368	−0.002	1.334	0.034
$R(C^8,O^9)$	1.228	1.227	0.001	1.228	0.001	1.266	−0.038
$R(C^8,C^{10})$	1.506	1.514	−0.008	1.515	0.001	1.529	−0.014
$R(C^4,O^{11})$	1.415	1.401	0.014	1.389	−0.012	1.399	−0.010
$R(O^{11},C^{12})$	1.350	1.370	−0.020	1.405	0.035	1.394	0.011
$R(C^{12},O^{13})$	1.215	1.208	0.007	1.215	0.007	1.216	−0.001
$R(C^{12},C^{14})$	1.476	1.482	−0.006	1.458	−0.024	1.464	−0.006
$R(C^{14},C^{15})$	1.408	1.407	0.001	1.418	0.011	1.416	0.002
$R(C^{15},C^{16})$	1.380	1.386	−0.006	1.379	−0.007	1.381	−0.002
$R(C^{16},C^{17})$	1.400	1.396	0.004	1.412	0.016	1.411	0.001
$R(C^{17},C^{18})$	1.374	1.387	−0.013	1.374	−0.013	1.375	−0.001
$R(C^{18},C^{19})$	1.404	1.401	0.003	1.449	0.048	1.448	0.001
$R(C^{19},C^{14})$	1.406	1.413	0.007	1.461	0.048	1.460	0.001
$R(C^{19},O^{20})$	1.351	1.357	−0.006	1.268	−0.089	1.270	−0.002
Bond angles							
$A(C^1,C^2,C^3)$	119.6	119.8	−0.2	119.7	0.1	121.3	−1.6
$A(C^2,C^3,C^4)$	119.8	120.1	−0.3	120.5	−0.4	119.6	0.9
$A(C^3,C^4,C^5)$	121.4	120.7	0.7	120.0	0.7	119.7	0.3
$A(C^4,C^5,C^6)$	119.2	119.2	0	119.6	−0.4	120.6	−1
$A(C^5,C^6,C^1)$	120.5	120.8	−0.3	120.7	0.1	121.3	−0.6
$A(C^1,N^7,C^8)$	128.1	129.5	−1.4	129.6	−0.1	122.8	6.8
$A(N^7,C^8,C^{10})$	114.2	114.7	−0.5	114.9	−0.2	114.4	0.5
$A(N^7,C^8,O^9)$	123.9	123.6	0.3	123.6	0	129.0	−5.4
$A(C^4,O^{11},C^{12})$	117.2	118.2	−1	118.6	−0.4	118.5	0.1
$A(O^{11},C^{12},O^{13})$	122.0	122.0	0	119.3	2.7	119.9	−0.6
$A(O^{11},C^{12},C^{14})$	112.7	111.1	1.6	111.5	−0.4	111.7	−0.2
$A(C^{12},C^{14},C^{15})$	122.1	120.2	1.9	119.3	0.9	119.0	0.3
$A(C^{14},C^{15},C^{16})$	121.2	121.7	−0.5	122.7	−1	122.7	0
$A(O^{15},C^{16},O^{17})$	119.0	119.2	−0.2	118.5	0.7	118.4	0.1
$A(C^{16},C^{17},C^{18})$	121.1	120.3	0.8	120.8	−0.5	120.7	0.1
$A(C^{17},C^{18},C^{19})$	120.0	120.7	−0.7	123.3	−2.6	123.3	0
$A(C^{18},C^{19},O^{20})$	117.7	120.4	−2.7	119.9	0.5	120.0	−0.1
$A(C^{18},C^{19},C^{14})$	119.4	119.6	−0.2	114.7	4.9	114.7	0

[a] See Ref. [16]. [b] Algebraic deviations (Å, degrees) between experimental and theoretical values. [c] Algebraic deviations (Å, degrees) between theoretical values of the anion and molecule. [d] Algebraic deviations between theoretical values of the dianion and anion.

Table 5. NBO electronic charges q of the fragments of the species studied

Charge of the fragments	HO/O⁻	Ph	OCO	Ph	NH/N⁻	$COCH_3$
$q_{molecule}$	−0.17	0.21	−0.37	0.49	−0.22	0.06
q_{anion}	−0.71	−0.12	−0.43	0.45	−0.21	0.01
$q_{anion} - q_{molecule}$	−0.54	−0.33	−0.06	−0.03	0.01	−0.05
$q_{dianion}$	−0.73	−0.17	−0.42	0.28	−0.71	−0.26
$q_{dianion} - q_{dianion}$	−0.02	−0.05	0.01	−0.27	−0.50	−0.17

The charge change values $\Delta q = q_{anion} - q_{molecule}$ and $\Delta q = q_{dianion} - q_{anion}$ are usually quite informative in showing the distributions of the new charges in anions [8–13]. According to the present calculations the first (oxyanionic) charge remains localized mainly within the oxyphenylene fragment while the second (nitranionic) charge spreads over the acetanilide fragment.

CONCLUSION

The spectral and structural changes, caused by the conversion of the salophen molecule into the corresponding oxyanion and dianion have been studied by IR spectra DFT method at B3LYP/6-311++G** level. A comparison of calculated with measured infrared data can be used as a test for the reliability of the structural predictions for various molecules and anions of this and similar types. These predictions can be very useful in cases of molecules and ions for which experimental structural parameters are inaccessible or unknown. IR spectral changes, which take place as a result of the conversion of molecule into anions, were adequately predicted by the same theoretical method.

REFERENCES

1. P. Naumov, G. Jovanovski, S. Tancčeva, S. W. Ng, *Z. Anorg. Allg. Chem.*, 632, 454 (2006).
2. P. Tisovský, R. Šandrik, M. Horváth, J. Donovalová, J, J. Filo, M. Gáplovský, K. Jakusová, M. Cigáň, R. Sokolík, A. Gáplovský, *Molecules*, 22, 1961 (2017).
3. J. L. Castro, M. R. Lopez-Ramirez, J. F. Arenas, J. Soto, J.C. Otero, *Langmuir*, 28, 8926 (2012).
4. S. Y. Lin, H. L. Lin, Y. T. Chi, R. Y. Hung, Y. T. Huang, W. H. Hsieh, C. Y. Kao, *J. Pharm. Innov.*, 11, 109 (2016).
5. E. J. Baran, V. T. Yilmaz, *Coordin. Chem. Rev.*, 250, 1980 (2006)
6. I. N. Juchnovski, I. G. Binev, in: S. Patai, Z. Rappoport (Ed.): The chemistry of functional groups, Suppl. C., Wiley, New York, 1983, p. 107.
7. S. S. Stoyanov, J. A. Tsenov, D. Y. Yancheva, *J. Mol. Struct.*, **1009**, 42 (2012).
8. A. D. Popova, E. A. Velcheva, B. A. Stamboliyska, *J. Mol. Struct.*, **1009**, 23 (2012).
9. E. A. Velcheva, B. A. Stamboliyska, P. J. Boyadjiea, *J. Mol. Struct.*, **963**, 57 (2010).
10. A. D. Popova, M. K. Georgieva, O. I. Petrov, K. V. Petrova, E. A. Velcheva, *Int. J. Quant. Chem.*, **107**, 1752 (2007).
11. Ts. Kolev, E. Velcheva, B. Stamboliyska, *Bulg. Chem. Commun.*, **49**(D), 239 (2017).
12. E. Velcheva, Z. Glavcheva, B. Stamboliyska, *Bulg. Chem. Commun.*, **48**, 514 (2016).
13. E. Velcheva, B. Stamboliyska, S. Stoyanov, *Bulg. Chem. Commun.*, **49**(D), 137 (2017).
14. https://pubchem.ncbi.nlm.nih.gov/compound/1984
15. J. Stopek, *US Patent* 8 758 798 B2 (20014); D. Friedman, *US Patent* 9 186 324 B2(2015).
16. T. Maris, CCDC 779609: Experimental Crystal Structure Determination, Cambridge Crystallographic Data Centre, 2014.
17. B. B. Koleva, T. M. Kolev, M. Spiteller, *J. Pharm. Biomed. Analysis*, **46**, 267 (2008).
18. J. A. Bohmann, F. Weinhold, T. C. Farrar, *J. Chem. Phys.,* **1997**, 107, 1173.
19. M. J. Frisch, G. W. Trucks, H. B. Schlegel, G. E. Scuseria, M. A. Robb, J. R. Cheeseman, G. Scalmani, V. Barone, B. Mennucci, G. A. Petersson, H. Nakatsuji, M. Caricato, X. Li, H. P. Hratchian, A. F. Izmaylov, J. Bloino, G. Zheng, J. L. Sonnenberg, M. Hada, M. Ehara, K. Toyota, R. Fukuda, J. Hasegawa, M. Ishida, T. Nakajima, Y.Honda, O. Kitao, H. Nakai, T. Vreven, J.A. Montgomery, Jr., J. E. Peralta, F. Ogliaro, M. Bearpark, J. J. Heyd, E. Brothers, K. N. Kudin, V. N. Staroverov, R. Kobayashi, J.Normand, K. Raghavachari, A. Rendell, J. C. Burant, S. S. Iyengar, J. Tomasi, M. Cossi, N. Rega, J. M. Millam, M. Klene, J. E. Knox, J. B. Cross, V. Bakken, C. Adamo, J. Jaramillo, R. Gomperts, R. E. Stratmann, O. Yazyev, A. J. Austin, R. Cammi, C. Pomelli, J. W. Ochterski, R. L. Martin, K. Morokuma, V. G. Zakrzewski, G. A. Voth, P. Salvador, J. J. Dannenberg, S. Dapprich, A. D. Daniels, Ö. Farkas, J. B. Foresman, J. V. Ortiz, J. Cioslowski, D. J. Fox, Gaussian 09, Revision A1, Gaussian Inc., Wallingford CT, 2009.
20. A. D. Becke, *J. Chem. Phys.*, **98,** 5648 (1993).
21. C. Lee, W. Yang, G. R. Parr, *Phys. Rev.*, **B37,** 785 (1998).
22. J. Tomasi, M. Perisco, *Chem. Rev.*, **94,** 2027 (1994).
23. J. Tomasi, B. Mennucci, E. J. Cances, *J. Mol. Struct.*, *(THEOCHEM)*, **464** 211 (1999).
24. V. M. Vlasov, L. A. Oshkina, *Org. React.*, **28,** 47 (1993).
25. M. Szwarc, Ions and Ion Pairs in Organic Reactions, Wiley-Interscience, New York, 1972.

ИЧ СПЕКТРАЛНИ И СТРУКТУРНИ ПРОМЕНИ, ПРИЧИНЕНИ ОТ ПРЕВРЪЩАНЕТО НА САЛОФЕН В АНИОН И ДИАНИОН

С. С. Стоянов, Е. А. Велчева, Б. А. Стамболийска*

Лаборатория „Структурен органичен анализ", Институт по органична химия с център по фитохимия, Българска академия на науките, ул. „Акад. Г. Бончев", бл. 9, 1113 София

(Резюме)

Структурите на салофена, неговите анион и дианион са изследвани с помощта на ИЧ спектроскопия и DFT пресмятания. Ефектът на разтворителя е отчетен по метода на самосъгласуваното реактивно поле (IEFPCM). Намерено е добро съответствие между теоретичните и експерименталните вибрационни характеристики на изследваните частици. Използваният теоретичен метод добре предсказва силните спектрални промени, които съпътстват превръщането на салофена в анион и дианион. Установените структурни промени при тези превръщания са също значителни. Анализът на промените в атомните заряди показва, че първият (оксианионен) заряд остава локализиран в оксифениленовия фрагмент, а вторият (азанионен) заряд се делокизира върху ацетанилидния фрагмент.